Spin Density Distribution and Electronic Structure of Radical Anions of Ladder-type Oligorylenes

M. Baumgarten,* K.-H. Koch, and K. Müllen*

Contribution from the Max-Planck-Institut für Polymerforschung, Ackermannweg 10, D-55 128 Mainz, Germany

*Received November 9, 1993**

Abstract: The radical anions of ladder-type oligorylenes have been obtained from a homologous series of soluble oligoperinaphthylenes and characterized by EPR and ENDOR spectroscopy. By these methods in combination with HMO/McLachlan and PPP calculations and isotopic labeling, all ^1H hyperfine coupling constants have been assigned to the individual positions in the molecules. Considerable spin density prevails at both ends of the oligoperinaphthylenes, making them ideally suited as building blocks in molecular electronics. In higher oligomers, a redistribution of the position of highest spin density to more inner naphthalene units is predicted theoretically. The experimental and theoretical results point to a close relationship to even polyenes, but with the more rigid polyperinaphthylenes possessing a much lower band gap. The spin density distribution within the oligomers is in contrast to that of linear conjugated π-systems with phenyl end groups like oligo(*p*-phenylenevinylenes) and diphenylpolyenes, where the positions of highest spin density occur in the central parts of the molecules already for small oligomers. The chain length dependence of the spin density distribution and the largest ^1H hyperfine coupling constants are compared to data from optical absorption measurements of the neutral and monocharged species. While the former reflects the spin density at certain positions of the π-system, the latter characterize the whole conjugated chromophore.

Introduction

Organic molecules, which serve as media for the storage and transfer of charge, have been of great interest in recent years.[1-10] One reason for this is that charge passing through a molecule can be used for processing signals in electrical circuits, and another reason is that charge-transport mechanisms are important for the description of electrically conducting conjugated polymers.[11-14] Major questions within the latter area of research are whether the charged excitations carry a spin and what the spin density distribution is along a π-chain.[15-17] Theoretical and experimental studies of linear conjugated polymers point toward an effective conjugation length extending only over a limited number of repeating units.[18] In many cases it is not clear, however, whether these findings can be attributed to structural defects or, e.g., to twisted conformations of the subunits. Two systematic studies of the spin density distribution in the radical anions of oligo(*p*-phenylenevinylenes) in solution and in the solid state have been published.[19,20] They reveal a limit of spin density distribution over 5–8 repeat units, with position of highest spin density in the central double bonds.

Charged states can be produced not only by partial oxidation or reduction but also by optical excitation. Thus, irradiation of extended π-systems such as di(9-anthryl)-substituted polyenes creates electronic states which are almost localized at the terminal anthryl groups.[21] This effect is ascribed to a steric hindrance

Chart 1

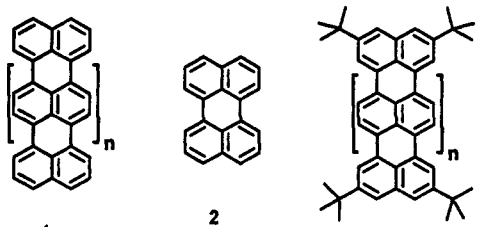

1 2

3: n=0
4: n=1
5: n=2
6: n=3

* Abstract published in *Advance ACS Abstracts*, June 15, 1994.

(1) (a) Baumgarten, M.; Huber, W.; Müllen, K. *Adv. Phys. Org. Chem.* **1993**, *28*, 1–44. (b) Baumgarten, M.; Müllen, K. *Top. Curr. Chem.* **1994**, *169*, 1–103.

(2) (a) Arrhenius, T. S.; Blanchard-Desce, M.; Dvolaitzky, M.; Lehn, J. M.; Malthete, J. *Proc. Natl. Acad. Sci. U.S.A.* **1986**, *85*, 5355–5359. (b) Lehn, J. M. *Angew. Chem., Int. Ed. Engl.* **1988**, *27*, 89–113.

(3) Effenberger, F.; Schlosser, H.; Bäuerle, P.; Maier, S.; Port, H.; Wolf, H. C. *Angew. Chem., Int. Ed. Engl.* **1988**, *27*, 281–284.

(4) Leitner, A.; Lippisch, M. E.; Draxler, S.; Riegler, M.; Aussenegg, F. R. *Appl. Phys.* **1985**, *B36*, 105–109.

(5) Miller, J. R.; Calcaterra, L. T.; Closs, G. L. *J. Am. Chem. Soc.* **1984**, *106*, 3047–3049.

(6) Heitele, H.; Michel-Beyerle, M. E. *J. Am. Chem. Soc.* **1985**, *107*, 8286–8288.

(7) Schmidt, J. A.; Siemiarczuk, A.; Weedon, A. C.; Bolton, J. R. *J. Am. Chem. Soc.* **1985**, *107*, 6112–6114.

(8) Gust, D.; Moore, T. A.; Lidell, P. A.; Nemeth, G. A.; Makings, L. R.; Moore, A. L.; Barrett, D.; Pessiki, P. J.; Bensasson, R. V.; Rougee, M.; Chachaty, C.; Schryver, F. C.; Van der Auweraer, M.; Holzwarth, A. R.; Connolly, J. S. *J. Am. Chem. Soc.* **1987**, *109*, 846–856.

(9) Beratan, D. N. *J. Am. Chem. Soc.* **1986**, *108*, 4321–4326.

(10) Joachim, C.; Launay, J. P. *J. Mol. Electron.* **1990**, *6*, 37–50.

(11) Wudl, F. The Chemistry of Organic Conductors. A review of Strategies. In *The Physics and Chemistry of Low Dimensional Solids*; Alcacer, Ed.; L. Reidel: Boston, MA, 1980; pp 265–291.

(12) Chance, R. R.; Boudreaux, D. S.; Brédas, J. L.; Silbey, R. In *Handbook of Conducting Polymers*; Skotheim, T. A., Ed.; Dekker: New York, 1986; pp 825 ff.

(13) Brédas, J. L. In *Handbook of Conducting Polymers*; Skotheim, T. A., Ed.; Dekker: New York, 1986; pp 859 ff.

(14) Friend, R. H.; Bradley, D. D. C.; Townsend, P. D. *J. Phys. D., Appl. Phys.* **1987**, *20*, 1367–1384.

(15) Colaneri, N. F.; Bradley, D. D. C.; Friend, R. H.; Spangler, C. W. In *Springer Series in Solid-state Sciences, Electronic Properties of Conjugated Polymers III*; Kuzmany, H., Mehring, M., Roth, S., Eds.; Springer-Verlag: Berlin, 1989; Vol. 91, pp 91–95.

(16) Shen, Y. Q.; Lindenberger, H.; Bleier, H.; Roth, S. *Springer Series in Solid-state Sciences, Electronic Properties of Conjugated Polymers III*; Kutzmany, H.; Mehring, M., Roth, S., Eds.; Springer-Verlag: Berlin, 1989; Vol. 91, pp 96–99.

(17) Mehring, M.; Grupp, A.; Höfer, P.; Käss, H. *Synth. Met.* **1989**, *28*, D399–D406.

(18) Prasad, P. N. In *Organic Materials for Non-linear Optics*; Hann, R. A., Bloor, D., Eds.; The Royal Society of Chemistry: London, 1989; pp 264–274.

(19) Schenk, R.; Ehrenfreund, M.; Huber, W.; Müllen, K. *J. Chem. Soc., Chem. Commun.* **1990**, 1673–1675.

(20) Brendel, P.; Grupp, A.; Schenk, R.; Mehring, M.; Müllen, K. *Synth. Met.* **1991**, *45*, 49.

(21) Heine, B.; Sigmund, E.; Maier, S.; Port, H.; Wolf, H. C.; Effenberger, F.; Schlosser, H. *J. Mol. Electron.* **1990**, *6*, 51–60.

0002-7863/94/1516-7341$04.50/0

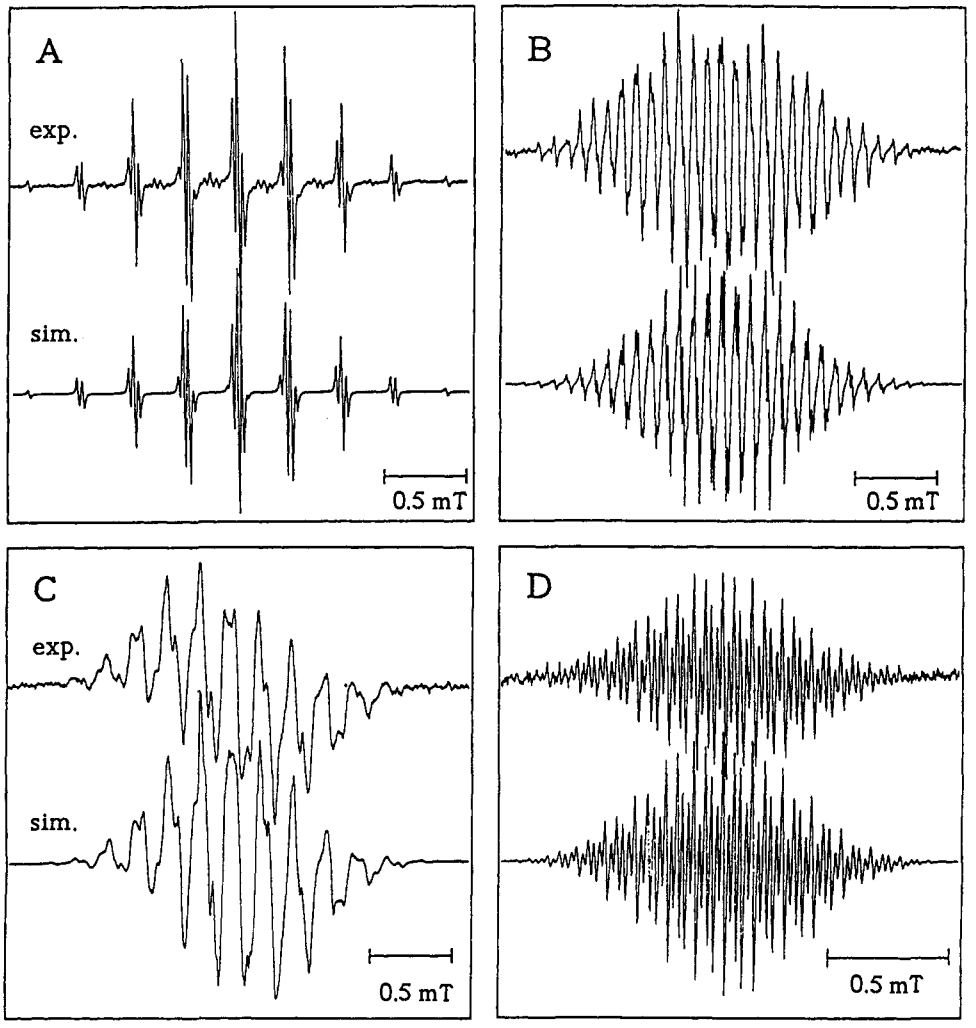

Figure 1. EPR spectra and computer simulation of the substituted perylene $3^{\bullet-}$ (A), terrylene $4^{\bullet-}$ (B), quaterrylene $5^{\bullet-}$ (C), and $5^{\bullet 3-}$ (D) in THF. EPR conditions: microwave frequency, 9.55 GHz; *T*, 230 K.

between the anthryl moiety and the polyene chain. The problem of undefined geometry could be overcome by using fully conjugated, rigid, planar π-systems as model compounds. We have, therefore, chosen well-defined oligoperinaphthylenes **3–6** (Chart 1).[22,23]

The structurally related polymer **1** (polyperinaphthylene, PPN) has attracted great attention since it is predicted theoretically to possess a low band gap.[12,13,24,25] Previous efforts toward the preparation of polymer **1** have included cationic cyclization,[26] pyrolytic treatment,[27,28] and plasma polymerization[29] of suitable precursors. Such drastic conditions, however, led to partially graphitized, irregular structures. The number of defects was consequently very large, and structurally well-defined materials could not be obtained.

Charged derivatives of the soluble, *tert*-butyl-substituted oligomers **3–6** with $n = 0$–3, on the other hand, should offer the possibility of testing the charge (spin) density distribution as a function of the size of the planar π-system.

We have studied the electron spin delocalization in radical anions of ladder-type oligoperinaphthylenes **3–6**, also called oligorylenes.[30,31] The determination of the spin distribution in the radical anions of oligorylenes should allow the study of "pure" electronic effects such as the formation of partially localized states. Justification for this approach comes from the fact that both optical excitation and chemical doping under formation of charged excitations can lead to enhanced conductivity of conjugated polyenes.[32,33] Therefore, an attempt is made also to correlate optical and EPR/ENDOR data in the study of the radical anions and chain length-dependent effects.

Results

The EPR spectrum of the radical anion of 2,5,8,11-tetra-*tert*-butylperylene (**3**) (Figure 1A) is quite similar to that of the unsubstituted perylene (**2**) anion, which is a long known standard for EPR spectroscopy.[34,35] The EPR spectrum of $3^{\bullet-}$ shows nine sets of hyperfine (hf) lines, which are caused by two sets of four

(22) Bohnen, A.; Koch, K.-H.; Lüttke, W.; Müllen, K. *Angew. Chem., Int. Ed. Engl.* **1990**, *29*, 525–527.
(23) Koch, K.-H.; Müllen, K. *Chem. Ber.* **1991**, *124*, 2091–2100.
(24) Tyutyulkov, N.; Tadjer, A.; Mintcheva, I. *Synth. Met.* **1990**, *38*, 313.
(25) (a) Baumgarten, M.; Karabunarliev, S.; Koch, K.-H.; Müllen, K.; Tyutyulkov, N. *Synth. Met.* **1992**, *47*, 21–36. (b) Viruela-Martin, P.; Viruela-Martin, P. M.; Orti, E. *J. Chem. Phys.* **1992**, *97*, 8470.
(26) Banning, J. H.; Jones, M. B. *Polym. Prepr., Am. Chem. Soc., Div. Polym. Chem.* **1987**, *28*, 223–224.
(27) Murakami, M.; Yoshimura, S. *Mol. Cryst. Liq. Cryst.* **1985**, *118*, 95–102.
(28) Iqbal, Z.; Ivory, D. M.; Marti, J.; Brédas, J. L.; Baughman, *Mol. Cryst. Liq. Cryst.* **1985**, *118*, 103–110.
(29) Murashima, M.; Tanaka, K.; Yamabe, T. *Synth. Met*, **1989**, *33*, 373–380.
(30) Clar, E. *Chem. Ber.* **1948**, *81*, 52–63.
(31) Clar, E.; Kelly, W.; Laird, R. M. *Monatsh. Chem.* **1956**, *87*, 391.
(32) Karl, N. In *Crystal, Growth, Properties and Applications*; Freyhardt, H. C., Ed.; Springer Verlag: Berlin, 1980; Vol 4.
(33) Conwell, E. M.; Jeyadev, S. *Synth. Met.* **1989**, *28*, 229–258.
(34) Colpa, J. P.; Bolton, J. R. *Mol. Phys.* **1963**, *6*, 273–282.
(35) Gerson, F. In *Hochauflösende* ESR-Spektroskopie; Foerst, W., Gruenewald, H., Eds.; Verlag Chemie: Weinheim, Germany, 1967; English Edition, 1970.

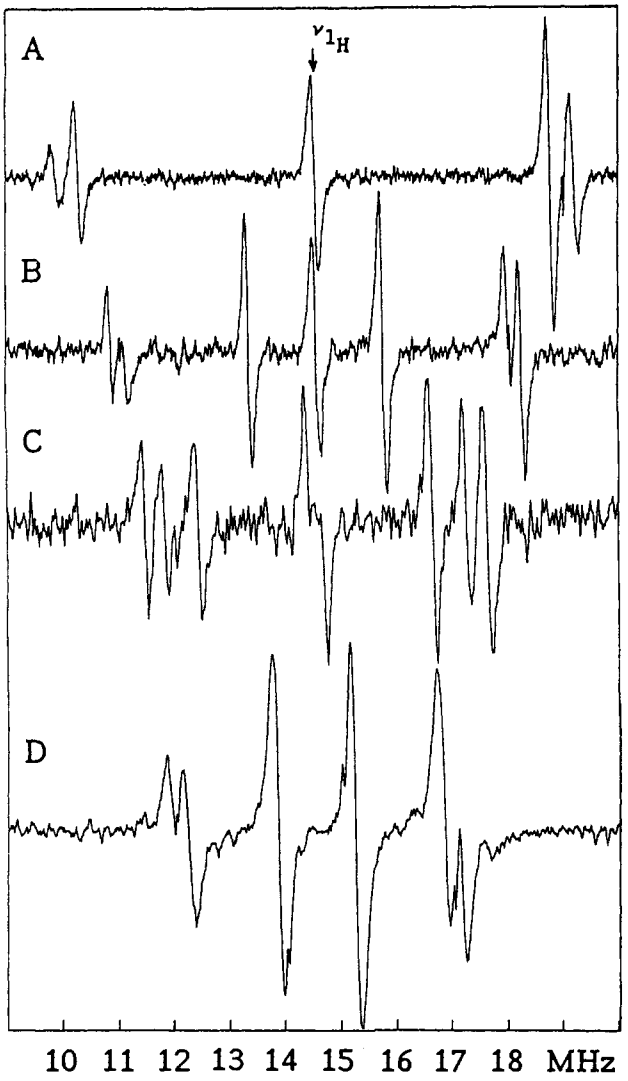

Figure 2. ENDOR spectra of perylene $3^{\bullet-}$ (A), terrylene $4^{\bullet-}$ (B), quaterrylene $5^{\bullet-}$ (C), and pentarylene $6^{\bullet-}$ (D). ENDOR conditions: microwave frequency, 9.55 GHz; *T*, 220 K; microwave power, 10–20 mW; radiofrequency power, 50–100 W.

equivalent proton couplings in the 1 and 3 positions. In addition, small ^{13}C signals from ^{13}C nuclei in natural abundance (1.1%) are obtained.

The ENDOR[36] spectrum of $3^{\bullet-}$ given in Figure 2A shows two large proton couplings, which are not totally separated, and an additional signal at the proton Larmor frequency (ν_{1H}), which is due to the nine protons of each *tert*-butyl group at the four equivalent positions 2. With the experimentally determined hyperfine couplings (hfcs) and the given multiplicity, the computer simulation of the experimental spectrum is straightforward. The assignment of the individual proton couplings is taken in analogy to the perylene anion radical and in agreement with the HMO/McLachlan approach.[37]

The radical anion of the terrylene derivative $4^{\bullet-}$, in which the π-system is extended by one naphthylene unit, already exhibits a complex EPR spectrum (Fig. 1B). The hyperfine couplings can only be determined by ENDOR spectroscopy (Figure 2B), with two large ^1H couplings for positions 1 (0.248 mT) and 3 (0.265 mT) and a smaller one for position 7 (0.087 mT), the central protons. The measured hf couplings allow satisfactory computer simulation of the experimental EPR spectrum (Figure 1B).

(36) Kurreck, H.; Kirste, D.; Lubitz, W. *ENDOR of Radicals in Solution*; Methods in Stereochemical Analysis; VCH Publishers, Inc.: Weinheim, FRG, 1988.
(37) McLachlan, A. D. *Mol. Phys.* **1960**, *3*, 233–252.

Table 1. ^1H Hyperfine Coupling Constants from ENDOR Measurements and HMO/McLachlan and PPP Calculations

		experimental		calculated			
radical	pos.	a_{exp} (mT)	n^a	ρ_π	a_{HMO} (mT)^b	$\rho_\pi{}^c$	a_{PPP} (mT)^b
$2^{\bullet-}$	1	0.308[d]	4	0.107	0.25	0.114	0.26
	2	0.046[d]	4	–0.023	–0.05	–0.044	–0.10
	3	0.353[d]	4	0.153	0.35	0.181	0.41
$3^{\bullet-}$	1	0.302	4	0.107	0.25	0.114	0.26
	3	0.332	4	0.153	0.35	0.181	0.41
$4^{\bullet-}$	1	0.248	4	0.096	0.22	0.113	0.26
	3	0.265	4	0.114	0.26	0.141	0.32
	7	0.087	4	0.027	0.06	0.019	0.44
$5^{\bullet-}$	1	0.194	4	0.082	0.19	0.100	0.23
	3	0.219	4	0.091	0.21	0.112	0.26
	7	0.013	4	–0.002	–0.01	–0.014	–0.03
	8	0.151	4	0.044	0.10	0.051	0.12
$6^{\bullet-}$	1	0.163	4	0.070	0.16	0.086	0.19
	3	0.185	4	0.076	0.17	0.091	0.21
	7	0.050	4	–0.007	–0.02	–0.027	–0.07
	8	0.163	4	0.047	0.11	0.063	0.14
	9	0.050	4	0.019	0.04	0.014	0.03
$7^{\bullet-}$	1/6	0.108	4	0.019	0.05		
	2/5	0.038	4	0.023	0.06		
	4	0.128	2	0.039	0.09		
	7/12	0.151	4	0.071	0.16		
	9/10	0.188	4	0.084	0.19		
$5^{\bullet 3-}$	1	0.072	4	0.027	0.06	0.00	0.03
	3	0.119	4	0.075	0.17	0.083	0.19
	7	0.235	4	0.083	0.19	0.11	0.25
	8[e]	–0.049	4	–0.012	–0.03	–0.031	–0.07

[a] Multiplicity of the protons. [b] $Q = 2.29$ mT. [c] PPP-CI calculations.[42] [d] Reference 30. [e] General TRIPLE measurements.

General TRIPLE measurements[38] yield the same sign for the three hf couplings, in accordance with the HMO/McLachlan calculations[37] (Table 1) for the 30 π-centers, which are also used for assignment. The McLachlan calculations give the spin density ρ at the corresponding carbon centers, from which the proton hyperfine couplings are calculated by the McConnell relation:[39]

$$a(\mathrm{H}) = Q\rho$$

with $Q = 2.29$ mT.[40,41]

A further reduction to a paramagnetic trianion is not observed; the final dianion stage of reduction, $4^{2-}/2K^+$ is diamagnetic and therefore accessible to NMR spectroscopy.[23]

The "tetrameric" pericondensed naphthylene system quaterrylene (**5**) can be reduced to the monoanion and even through the dianion into the trianion radical by prolonged contact with a potassium mirror:

$$5 \xrightarrow{+e^-} 5^{\bullet-} \xrightarrow{+e^-} 5^{\bullet 2-} \xrightarrow{+e^-} 5^{\bullet 3-}$$

First, an EPR spectrum of $5^{\bullet-}$ with 13 relatively broad sets of hf lines is detected (Figure 1C). The ENDOR spectrum of this monoanion species shows three large proton couplings and a pair of lines at ν_{1H}. The comparison with HMO/McLachlan calculations confirms the assumption that the largest couplings are still due to the protons at positions 1 and 3, while the ^1H hfc of position 8 is intermediate, with $a(H) = 0.151$ mT (Table 1).

Further reduction of the anion radical leads to a new EPR spectrum that is characterized by very sharp lines and a much smaller total field width. Also, the ENDOR spectrum of the anion radical differs from that of the monoanion and indicates

(38) Biehl, R.; Plato, M.; Möbius, K. *J. Chem. Phys.* **1975**, *63*, 3515–3522.
(39) (a) McConnell, H. M. *J. Chem. Phys.* **1956**, *24*, 632. (b) McConnell, H. M.; Chesnat, D. B. *J. Chem. Phys.* **1958**, *28*, 107–117.
(40) *Q*-value of 2.29 mT adopted for the radical anion of perylene.
(41) Of course, within this simple approach, the *Q*-value of the McConnell equation is kept constant for the homologous series.

Chart 2

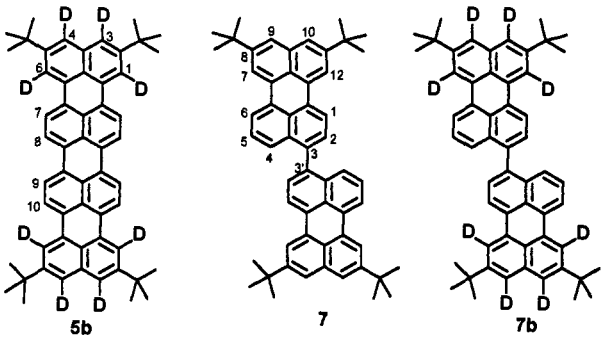

some spin density redistribution in the more highly charged species $5^{\bullet 3-}/3K^+$. General TRIPLE measurements allow determination of a different sign for the smallest hf coupling (Table 1 bottom).

It is not possible to differentiate between protons at different carbon positions by the number of equivalent protons due to the symmetry of the molecules. Therefore, independent experimental evidence for the given assignment stems from measurements of isotopically labeled material. Partially deuterated quaterrylene **5b** (Chart 2) was prepared by use of naphthalene-d_8 for the two outermost aryl units and standard binaphthylene for the central unlabeled unit[23] (see Experimental Section). During the synthetic procedures, including anionic and cationic cyclization conditions, some reprotonation occurred, leading to a final deuterium contant of ca. 70% for positions 1 and 3.

The ENDOR spectrum of the anion radical, therefore, still shows two proton couplings of 0.219 and 0.194 mT, but their intensities relative to the smaller proton coupling of 0.151 mT for the inner position 8 are drastically reduced (Figure 3). Additional support for the assignment stems from a pair of lines symmetrically centered at the free deuterium frequency. This deuterium coupling of 0.032 mT is not further resolved and corresponds to a proton coupling of 0.206 mT (Figure 3), which is just the average of the two resolved proton hfcs.

The spin distribution in quaterrylene may nicely be compared to that in anion radicals of singly bridged 2,2',5,5',8,8',9,9'-octa-*tert*-butyl-3,3'-biperylene (**7**, Chart 2) with the same number of π-centers. Here the question arises of whether the torsion of the subunits leads to independent perylene electrophores or to a complete conjugation with spin delocalization in the monocharged state. The optical absorption measurements of the neutral compound **7** show only a very small bathochromic shift, which could be induced by the substitution at the 3 position, compared to the same data for perylene (λ_{max} 451 (**7**) and 445 nm (**3**)) and point toward a hindered conjugated between the two perylenyl electrophores in **7**. The EPR spectrum of **7** in THF or 2-methyltetrahydrofuran (MTHF) changes with the concentration of monoradical and counterion. After short reduction with low yields of monoradical (weakly reduced stage), the EPR spectrum of $7^{\bullet -}$ in THF exhibits a 15-line hyperfine pattern due to 14 protons at positions of high spin density, and the corresponding ENDOR spectrum reveals at least six proton couplings, where the largest one is nearly half as large as that for perylene itself (Figure 4A,B). Thus the electron spin is effectively delocalized over the entire molecule within the time scale of the EPR/ENDOR experiment. Upon lowering the temperature or increasing the monoradical concentration versus neutral compound (with higher counterion concentration), the spectrum changes to one with an alternating line width pattern. Thereby, every second line becomes more intense with additional resolution, until, in the frozen state or after transformation of all neutral molecules into the monoradical form, only an 8-line pattern from seven large proton hfcs is obtained (Figure 4A). The sizes of the hfcs are then comparable to those of perylene, with proton hyperfine couplings of 0.357, 0.319, and 0283 mT. Thus, at low

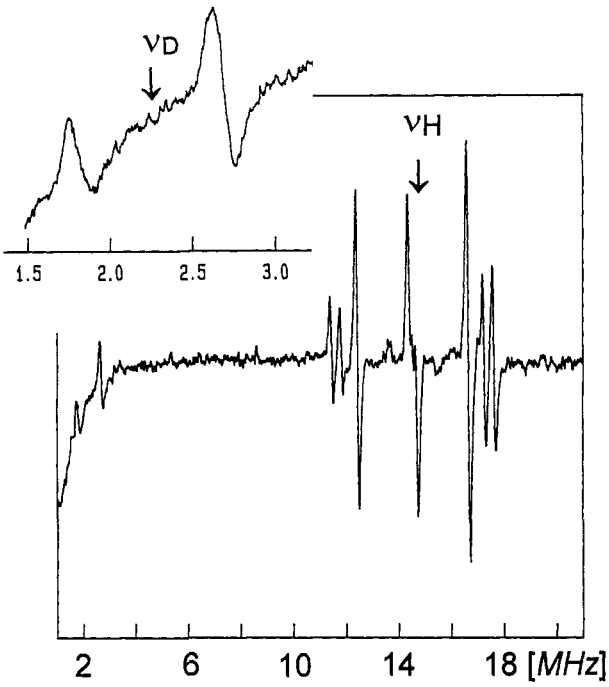

Figure 3. ^{1}H- and ^{2}H-ENDOR spectrum of deuterated quaterrylene $5b^{\bullet -}$ in THF. Inset: an enhanced deuterium spectrum.

temperatures (frozen solution) or higher monoradical and counterion concentrations, a localized spin density distribution on one perylenyl unit results (Figure 4A, bottom).

To confirm the assignment of the proton couplings to the individual proton positions resulting from HMO/McLachlan calculations, measurements were performed on the partially deuterated 7,7'-9,9'-10,10'-12,12'-deutero-3,3'-biperylene (**7b**, Chart 2). As already suggested from the calculations, the delocalized monoanion of **7b** shows a drastic decrease of the two largest proton couplings which, therefore, must be assigned to the deuterated positions (H–D exchange > 80%). Again, new deuterium couplings are detected in the low-frequency ENDOR spectrum which correlate to the two nearly vanishing proton couplings by the gyromagnetic ratio γ_D/γ_H. Thus, even in this singly bridged π-system, the spin density distribution is similar to the one in $5b^{\bullet -}$, with highest spin density in the peri positions 9,9' and 10,10'. The mixed spectra obtained from simultaneous existence of both species, localized and delocalized, can be simulated at each particular temperature by accounting for the appropriate intensity ratio. Therefore, it is difficult to decide whether we are dealing with an electron transfer between two perylene units in the ground state of the monoanion or if the thermodynamic equilibrium between the two species is changed upon variation of the experimental conditions.

For the radical anion of the pentarylene derivative $6^{\bullet -}$ only a broad signal with weakly resolved shoulders could be measured by EPR. The ENDOR spectra, however, yield three pairs of lines for the different positions (Figure 2C). The largest coupling is given with 0.185 mT (for comparison, 0.235 mT for $5^{\bullet -}$) and must be assigned to position 3, while eight protons from position 1 (and 6, 13, 18) and position 8 (and 11, 20, 25) contribute to the hfc of 0.165 mT. Additional PPP calculations[42] (see Table 1) support the final assignment. Further reduction leads to a change of the fine structure overlaying the broad EPR signal, and the ENDOR spectrum shows a new large ^{1}H coupling of 0.22 mT, indicating also the formation of a stable trianion radical (not shown).

In order to verify the particular redox states and to compare the changes of the hyperfine couplings with another, independent

(42) PPP-CI calculations taking all single excited configurations into account and a convergence criterion of $\Delta E = 5 \times 10^{-7}$.

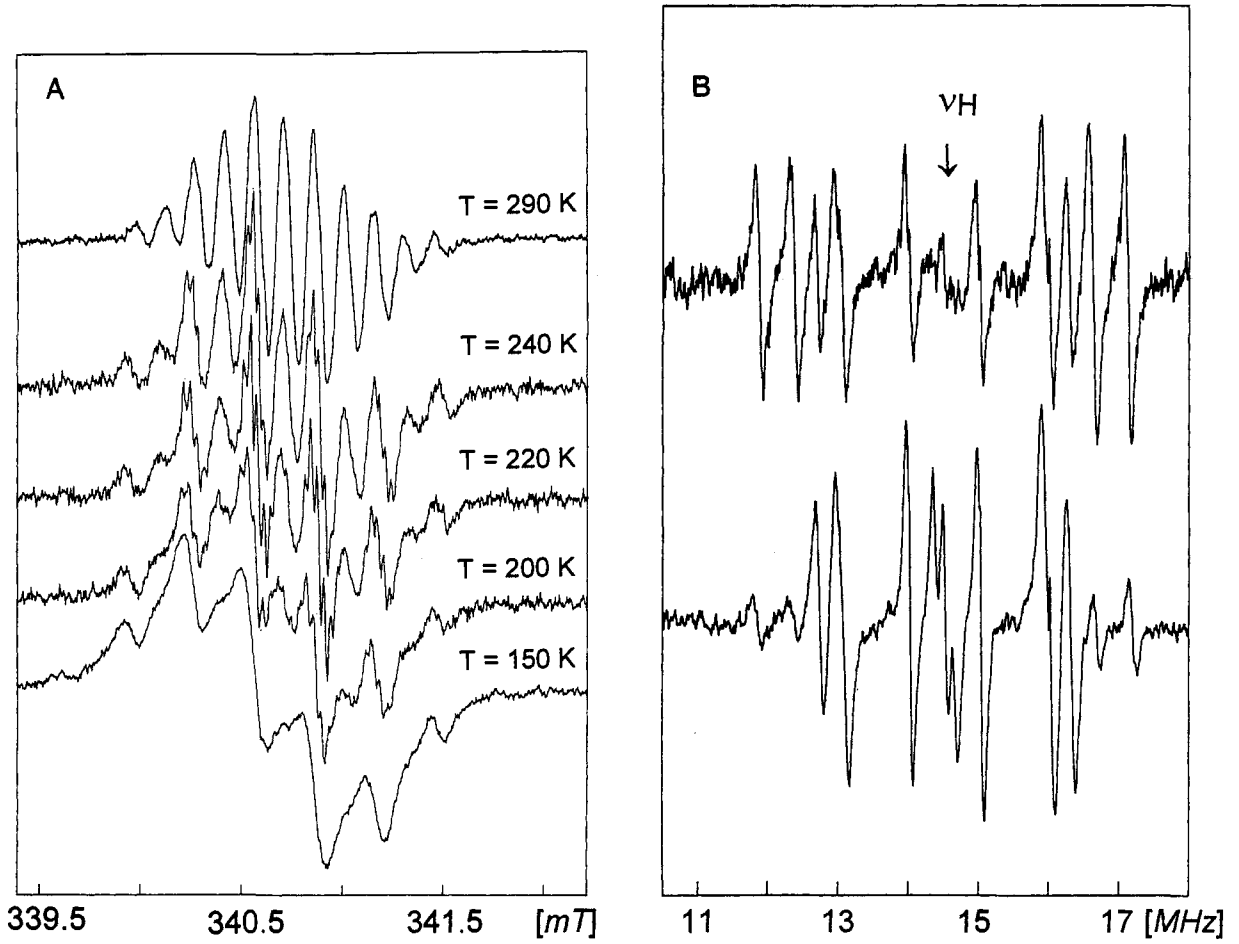

Figure 4. (A) Temperature-dependent EPR spectra of $7^{\bullet-}$. (B) ENDOR spectrum of 3,3′-biperylene ($7^{\bullet-}$ and 3,3′-biperylene-d_8 ($7b^{\bullet-}$) in THF.

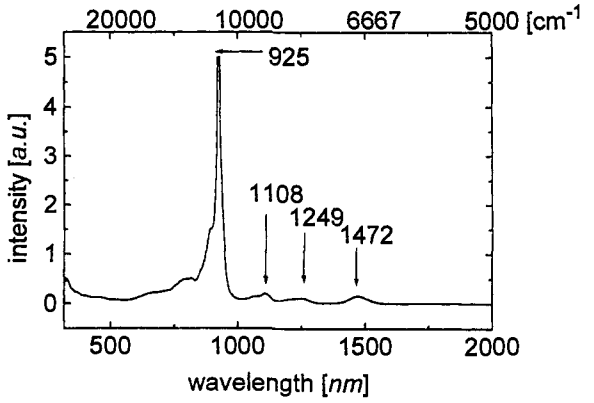

Figure 5. Vis/near-IR absorption spectrum of the radical anion of quaterrylene $5^{\bullet-}$ THF.

property of the electrophore, we also studied the chain length-dependent shifts in the optical absorption bands of the monoanions. While the neutral compounds exhibit several sharp absorptions with increasing intensity up to λ_{max} (due to vibronic couplings), the monoanions of the series **3–6** exhibit one dominating strong absorption peak together with 3–4 weak and broad bathochromically shifted absorptions (Figure 5 and Table 2). These weak absorptions at long wavelength disappear upon reduction to the dianion, while the strong absorption in the visible region is shifted only slightly to smaller wavelengths.

Discussion

The evaluation of the ^{1}H hyperfine couplings from EPR and additional ENDOR measurements together with computer simulations of the EPR spectra is straightforward. The four *tert*-butyl groups at positions 2 lead to a drastic enhancement in solubility, but their electronic influence on the π-systems is very small, as shown by direct comparison of $2^{\bullet-}$ and $3^{\bullet-}$. The similarity of $3^{\bullet-}$ and unsubstituted perylene radical anion $2^{\bullet-}$ can be explained by the low spin density at position 2, to which the substituents are attached. In general, the measured hyperfine couplings are slightly smaller in $3^{\bullet-}$ than in the nonsubstituted perylene $2^{\bullet-}$,[34,35] as given in Table 1.

Table 2. Optical Absorption Data [λ_{max} (eV)] for Neutral and Monocharged Rylenes **3–6** in THF, Respectively[a]

compd	neutral	monoanion
3	2.78	2.14; 1.65
4	2.21	1.60; 1.09
5	1.87	1.34; 0.84
6	1.66	1.16; 0.68

[a] For the monoanions are given two values, the first for the most intense band dominating the spectrum, and the second for the weak absorptions of longest wavelength (see Figure 5).

The assignments of the experimentally determined hfcs of the homologous radical anions are in line with HMO/McLachlan and PPP-CI calculated spin densities and are verified additionally by the deuterium labeling for $5^{\bullet-}$. The assignments adopted in Table 1 are thus beyond doubt. Assignment problems arise only for the higher charged species, for example the trianions $5^{\bullet 3-}$ and $6^{\bullet 3-}$.

The good agreement between calculated and measured hf couplings and the independence of radical anion concentration rule out the possibility that counterion effects strongly influence the prevailing spin distribution. An effective delocalization due to an electron hopping between the end groups in the time scale of the experiment—as in the case of biperylene **7**, where the exchange between the two perylene subunits is only observed by

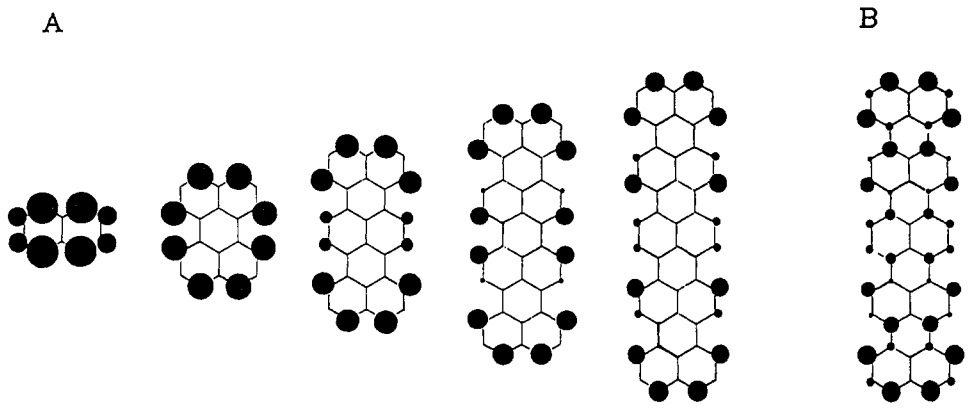

Figure 6. (A) Experimentally determined spin densities for the homologous series of the oligorylenes. (B) HMO/McLachlan analysis for pentarylene $6^{\bullet-}$ including quaternary centers. The size of the areas is proportional to the spin density.

EPR/ENDOR and not in the much faster optical absorption spectroscopy—can also be ruled out by parallel detection of the optical absorptions, which show a steady bathochromic shift with increasing number of repeat units. The absorption spectra of rylenes are thus consistent with truly delocalized species (see also discussion in ref 1a). Furthermore, the ENDOR spectra were taken at 220 K, where counterion effects are much weaker than at higher temperatures, as found from temperature dependence studies of the electronic absorption by Hoijtink et al.,[43] who found even smaller counterion effects with increasing size of the π-system. This is also supported by NMR studies of the dianion salts 3^{2-}/2K+ and 4^{2-}/2K+, where the variation of the counterion (Li^+ and K^+) does not change the chemical shifts significantly.[23]

Figure 6A illustrates the experimentally determined hf couplings for the different centers. The areas of the circles are directly proportional to the values of the measured hfcs. Also shown are the calculated spin densities from a HMO/McLachlan analysis[37,40] for the pentarylene radical anion $6^{\bullet-}$ (in the same scale) where the spin densities at the quaternary carbon atoms are included (see Figure 6B), which cannot be measured by EPR. The MO coefficients for the inner naphthalene carbon atoms (positions 4a, 8a) are vanishingly small because they lie on a nodal plane of the LUMO. The peri positions connecting the naphthalene units have smaller spin densities than those at positions 1 and 3 and support the interpretation of our experimental data.

Chain Length Dependence of Spin Density Distribution and Optical Energies. From the standpoint of symmetry, one is dealing with two different classes of oligomers: that with an even number of naphthalene units and that with an odd number. For both classes, the largest spin density is located at the peri position 3. That naphthalene itself does not fit well into this consideration is already seen from the comparison with perylene and terrylene, where new centers of large spin density occur at position 1. This is due to the changed symmetry of the frontier orbitals on going from naphthalene to perylene. The largest hf coupling, a_{max}, decreases from terrylene $4^{\bullet-}$ (0.265 mT) to pentarylene $6^{\bullet-}$ (0.185 mT), yielding a ratio of 1.43 instead of 1.67, which would be expected from the ratio of the number of π-centers (50/30), while the small coupling from the central positions 7 and 9 decreases from 0.087 to 0.050 mT. Combining both series, ratios a_{max}/a_{min} of 3.03 (0.265/0.087) and 3.70 (0.185/0.050) are found, thus indicating an relative increase of spin density on the outer naphthalene units. Nearly the same effect is found when comparing **3** and **5** with an even number of naphthalenes (20 vs 40 π-centers). For the largest hf coupling, the experiments provide values of 0.332 mT for $3^{\bullet-}$ and 0.219 mT for $5^{\bullet-}$. The ratio a_3/a_2 is 1.52 instead of 2.0, which would have been anticipated on simply doubling the number of π-centers.

In pentarylene, on the other hand, the spin density from position 8 at the next inner naphthylene unit has already reached the same size as that from position 1. Therewith some redistribution of spin is indicated. Spin density calculations by a PPP-CI procedure including geometry optimizations by the semiempirical AM1 and PM3 methods[44,45] suggests a spin density redistribution from position 3 to positions 1 and 8 in the higher oligomer hexarylene. Thus, for even larger π-systems, the position of highest spin density should be located in the more central naphthalene units. While the structural changes combined with charge uptake are most pronounced in the central part of the molecules, where partially quinoid structures are predicted, the spin density redistribution is also favored from energetic criteria, considering that the delocalization energy is a finite quantity and will be exceeded by the energetic costs of structural relaxation in long-chain conducting polymers (lattice distortion).[46-48]

The steady decrease of hyperfine couplings with increasing chain length immediately opens the questions of whether this physical property tends toward zero with increasing chain length and what would be the anticipated final value for a defect-free polymer when extrapolated to infinity. Therefore, the two largest hfcs are plotted versus $1/n_{eff}$,[49] where n_{eff} reflects the number of repeat units n corrected for a minor difference of the alkylated end groups by a constant $c = 0.2$ ($1/n_{eff} = 1/n + c$)[48,49] (see Figure 7A). The inverse dependence of absorption energies, redox potentials and hyperfine couplings is documented quite well in the literature.[19,20,48,49,50] The hfc does not approach zero, as would be expected for a complete delocalization, but hints of a final value of 0.07 ± 0.02 mT, indicating the limit of conjugation. This value is slightly smaller than that obtained from a Padé approximation,[51] considering the maximal hfcs of the three highest oligomers terrylene $4^{\bullet-}$, quaterrylene $5^{\bullet-}$, and pentarylene $6^{\bullet-}$ (a_{max} = 0.09 mT).

This convergence behavior of the maximum hfc may be compared to the data obtained from the optical absorption spectra of the neutral and monocharged compounds. When the optically determined transition energies are plotted versus the reciprocal number of naphthalene units ($1/n_{eff}$), a linear decrease with increasing n is obtained (Figure 7B). With the extrapolation of $1/n_{eff} = 0$, the HOMO–LUMO[48,50] energy gap ΔE for an infinite

(43) Buschow, K. H. J.; Dielmann, J.; Hoijtink, G. J. *J. Chem. Phys.* **1965**, *42*, 1993–1999.
(44) Stewart, J. J. P. MOPAC: A General Molecular Orbital Package (v. 6.00). *QCPE* **1990**, *455*, 10.
(45) (a) Karabunarliev, S.; Baumgarten, M.; Müllen, K.; Tyutyulkov, N. *Chem. Phys.* **1994**, *179*, 421–430. (b) Karabunarliev, S., to be published.
(46) Brédas, J. L.; Street, G. B. *Acc. Chem. Res.* **1985**, *18*, 309.
(47) Heeger, A. J.; Kivelson, S.; Schrieffer, J. R.; Su, W.-P. *Rev. Mod. Phys.* **1988**, *60*, 781–850.
(48) Tolbert, L. M. *Acc. Chem. Res.* **1992**, *25*, 561–568.
(49) Brédas, J. L.; Silbey, R.; Boudreaux, D. S.; Chance, R. R. *J. Am. Chem. Soc.* **1983**, *105*, 6555–6559.
(50) Hörhold, H. H.; Helbig, M. *Makromol. Chem. Macromol. Symp.* **1987**, *12*, 229–258.
(51) Jonson, R. C. In *Padé Approximation and their Application*; Graves-Morris, P. R., Ed.; Academic Press: London, 1973; pp 53 ff.

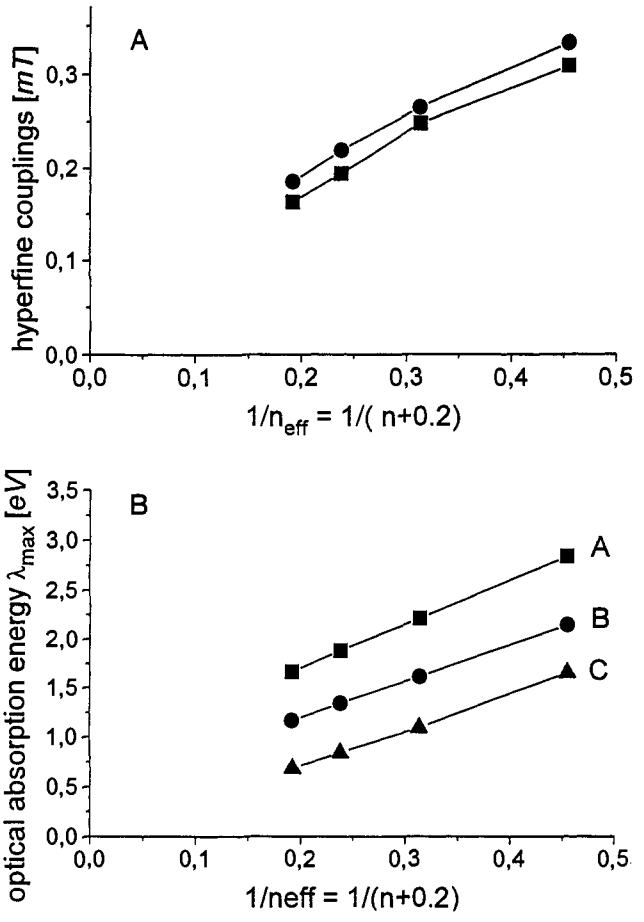

Figure 7. (A, top) Plot of the two largest hyperfine couplings versus $1/n_{eff}$; $n_{eff} = (1/n + 0.2)$, where n is the number of naphthalene units. (B, bottom) Plot of λ_{max} over $1/n_{eff}$ for the neutral forms (A, ■) and the monoanions of **3–6**, showing (B, ●) the most intense absorption and (C, ▲) the absorption at longest wavelength.

chain of a hypothetical defect-free polymer is obtained. In the case of polymer **1**, one of the lowest values for the energy gap—with $\Delta E = 0.8 \pm 0.1$ eV—is found so far for a neutral hydrocarbon polymer. This value of the energy gap is in the range of calculated energies for the band structure of **1**.[12,13,24,25] For the radical anions, the energy extrapolated from the $1/n_{eff}$ plot of the two transitions at long wavelength is much lower, corresponding to 0.1–0.5 eV (Figure 7B), depending on which of the two transitions, λ_{max} (maximum intensity) or λ_{max} (maximum wavelength), is used (Table 2). A polymer which is still soluble, on the other hand, cannot be synthesized by using alkyl groups at the chain end; therefore, for substantially higher oligomers to still be soluble, alkyl chains would need to be introduced on the repeat units,[52] where the electronic structure may differ slightly.

Comparison with Other π-Systems. Closely related to the rylenes are even polyenes. On the theoretical level oligorylenes can be viewed as two rigidly linked chains of *cis*-polyenes.[53] The McLachlan calculations also yield highest spin densities at both ends of the polyene chain, and for small soluble oligomers the measured hyperfine couplings can be explained well with this assignment.[54] Thus, polyenes with even numbers of carbon centers belong to the same type as the rylenes (type A). In these cases, the bond length variation leads to spin density localization in the more central part of the molecules only in very long π-chains, as also suggested by Bally et al.[55]

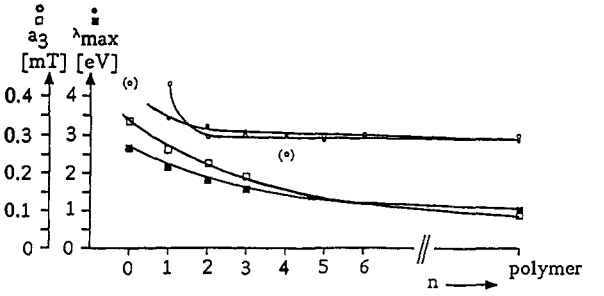

Figure 8. Plot of the largest hyperfine couplings a_3 from ENDOR spectroscopy (mT) of monoanions and λ_{max} values of neutral compounds from UV/vis absorption spectroscopy versus increasing chain length n (number of repeating units) for oligoperinaphthylenes **3–6** and oligo(*p*-phenylenevinylenes) (**8**), respectively. The value for the polymer was calculated with help of the Padé approximation.

Chart 3

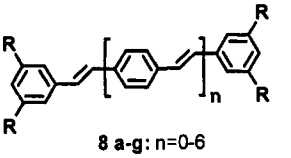

8 a-g: n=0-6

The situation of spin/charge density is completely changed in the case of odd polyenes, where either a neutral radical or charged states are created, which immediately show highest spin at the central positions (type B).[56] If the neutral phenyl end groups, on the other hand, are exchanged by pyridinium, an antisymmetric charge distribution and bond length alternation pattern results, with higher charge on one half of the molecule, which is explained by unstability of the symmetric stucture toward Peierls distortion.[57]

To investigate whether the parallel behavior of hyperfine couplings (spin densities) and λ_{max} values with increasing chain length can be generalized, we included the data of oligomers from *p*-phenylenevinylene **8** (Figure 8 and Chart 3). Indeed, the published data[19,58] show a different behavior, reaching a minimum after n = 5–8 for the largest hfc from the corresponding monoanions **8**$^{\bullet-}$ by ENDOR in THF solution. This difference compared to compounds **3–6** holds also for the plot of λ_{max} with increasing chain length. Additionally, the ENDOR data for **8**$^{\bullet-}$ reflect highest spin densities at positions in the central part of the molecule, in agreement with calculations (type B).

The difference in spin density distributions in oligomeric π-systems is attributed to their particular end groups, additional substituents, specific counterion localization, and size of the π-system.

Substituents like phenyl end groups on even oligoenes, which help in stabilizing soluble oligomers as in diphenyloligoenes, also shift the position of highest spin into the center of the oligoene chain. Thereby the radical anions of the smallest oligomers stilbene and diphenylbutadiene show the largest spin density in the central double bond(s) (type B), although the phenyl end groups are leading to a substantial increase of the conjugated chain, which is accounted for in the plots of absorption energy of neutral and anionic diphenyloligoenes versus $1/n_{eff}$ by a large constant c (c = 2.7–8).[47–49,56]

In radical ions of acenes (anthracene, tetracene, pentacene), the position of highest spin density resides in the center of the molecules as long as no specific end groups are used.[59] Previous reports on acene-type radical anions with benzoquinone end groups[60] have demonstrated that strong electron-withdrawing groups at the end may lead to spin localization of the unpaired

(52) Anton, U.; Müllen, K. *Makromol. Chem.* **1993**, *14*, 223–229.
(53) Brédas, J. L.; Baughman, R. H. *J. Chem. Phys.* **1985**, *83*, 1316–1322.
(54) Prasad, L. S.; Ding, R.; Bradford, E. G.; Kispert, L. D.; Wamd, H. *Isr. J. Chem.* **1989**, *29*, 33–38. (b) See also ref 1b, pp 26, 27.
(55) Bally, T.; Roth, K.; Tang, W.; Schrock, R. R.; Knoll, K.; Park, L. Y. *J. Am. Chem. Soc.* **1992**, *114*, 2440–2446.
(56) Tolbert, L. M.; Ogle, M. E. *J. Am. Chem. Soc.* **1990**, *112*, 9519–9527.
(57) Tolbert, L. M.; Zhao, X. *Synth. Met.* **1993**, *55–57*, 4788–4795.
(58) (a) Schenk, R, Gregorius, H., Müllen, K. *Adv. Mater.* **1991**, *3*, 492–493. (b) Schenk, R. Ph.D. thesis, Johannes Gutenberg-Universität, Mainz, FRG, 1990.
(59) Bolton, J. R.; Fraenkel, G. K. *J. Chem. Phys.* **1964**, *40*, 3307.

electron on one quinone end group moiety (e.g., in 2,3,9,10-tetramethyl-1,4,8,11-pentacenetetrone as compared to pentacene), while at elevated temperatures an electron exchange occurs, leading to an "effective delocalization" in the time scale of the EPR experiments.[60] This effect closely resembles our finding for the biperylene **7**, where spin localization at low temperatures is found on one perylene unit.

In oligothiophene radical cations, on the other hand, high prevailing spin densities are found at the two outermost α-positions (type A), a fact which is used for polymerization of oligomers.[60] Therefore, studies of well-defined oligomeric radical cations can be performed only in very dilute solution[62] or, e.g., in zeolite channels,[63] otherwise these reactive end groups have to be blocked by substituents, which may also lead to a spin density redistribution.[64]

Conclusion

We have experimentally observed the distribution of spin density in oligorylenes with increasing chain length n. In agreement with HMO/McLachlan/PPP-CI calculations and isotopic labeling, the radical anions of the oligomers still possess highest spin densities at the outermost naphthylene units, which makes them ideally suited as building blocks in molecular electronics for transfer of charge. A redistribution of spin density to more central naphthalene units should occur only in even higher oligomers. The extrapolation to the polymer **1** points toward a final value of 0.07 mT for the largest hyperfine coupling in a defect-free polymer.

The information on the conjugation from ENDOR studies is comparable to the data from optical absorption as shown for two examples, PPN and PPV. While ENDOR spectroscopy yields additional information on spin density distribution, the optical absorption data allow the determination of the optical band gap and the overall size of the conjugated π-system.

Experimental Section

The synthesis and characterization of the oligomers **3**, **4**, **5**, and **6** have been described in detail.[25] The newly prepared quaterrylene-d_8 **5b** and biperylene-d_8 **7b** were synthesized in analogy to **5** and **7**, respectively, starting from naphthalene-d_8 (99%, Cambridge Isotope Laboratories) for the two di-*tert*-butyl-substituted naphthalene end groups.[25] They were then transformed into the 2,7-di-*tert*-butyl-1-boronic acid-d_5 derivatives and coupled with 4,4′-dibromo-1,1′-binaphthyl to tetra-*tert*-butylternaphthyl, which was cyclized anionically to the biperylene **7b** (D:H > 85%) and finally cationically to **5b** (D:H ~ 70%). The final products **5b** and **7b** were characterized by NMR and UV/vis spectroscopy and mass spectrometry.

1,3,4,6,11,13,14,16-Octadeuterio-2,5,12,15-tetra-*tert*-butylquaterrylene (5b). ^{1}H NMR (500 MHz, $CDCl_3$): δ 8.31 (8H; 7-,8-,9-,10-,17-,18-,19-,20-H), 8.26 (weak, deuterio, 4H; 1-,6-,11-,16-H), 7.64 (weak, deuterio, 4H; 3-,4-,13-,14-H), 1.5 (s, 36H; $C(CH_3)$; D/H = 65%). MS-FD: m/e (relative intensity) 733 (25, $M^+ + 1$), 732 (55, M^+), 731 (75, $M^+ - 1$), 730 (100, $M^+ - 2$), 729 (75, $M^+ - 3$), 728 (55, $M^+ - 4$); D/H = 80%.

7,7′,9,9′,10,10′,12,12′-Octadeuterio-8,8′,11,11′-tetra-*tert*-butyl-3,3′-biperylene (7b). ^{1}H NMR (500 MHz, $CDCl_3$): δ 8.35–8.32 (d, 2H; J = 7.6 Hz, 1-,1′-H), 8.31–8.26 (d, weak deuterio; 4H; 7-,7′-,12-,12′-H), 8.22 (d, 1H; J = 1.9 Hz, 6-,6′-H), 8.20 (d, 1H; J = 1.9 Hz), 7.66 (d, 1H; J = 1.8 Hz), 7.53 (d, 2H; J = 7.7 Hz, 2-,2′-H), 7.33 (m, 4H, 4-,4′-,5-,5′-H), 1.51 (s, 18H; $C(CH_3)$), 1.49 (s, 18H; $C(CH_3)$); D/H = 90%. MS: m/e (relative intensity) 734 (100, M^+), 733 (80, $M^+ - 1$), 367 (60, $M^+/2$).

The radical anions of the *tert*-butyl-substituted rylenes were prepared in THF solutions on a potassium mirror under high vacuum in sealed glass tubes. Well-defined stages of reduction (monoanion, dianion, trianion, etc.) were reached by kinetic control and optical absorption measurements of the differently colored solutions.

EPR/ENDOR spectra in solution were recorded on a Bruker ESP300 spectrometer at X-band (9.54 GHz) frequency with 100-kHz field modulation.

Acknowledgment. We gratefully acknowledge support by the Bundesministerium für Forschung and Technologie and the Volkswagenstiftung. We thank Michael Schrohe for synthesis of the deuterated materials **5b** and **7b**, Lileta Gherghel for help in characterizing the radical anions by optical absorption spectroscopy, and Dr. Stoyan Karabunarliev for many helpful discussions and PPP-CI calculations.

(60) (a) Almlöf, J. E.; Feyereisen, M. W.; Jozefiak, T. H.; Miller, L. L. *J. Am. Chem. Soc.* **1990**, *112*, 1206–1214. (b) Rak, S. F.; Miller, L. L. *J. Am. Chem. Soc.* **1992**, *114*, 1388–1394.

(61) (a) Gill, R. E.; Malliaras, G. G.; Wildeman, J.; Hadziioannou, G. *Adv. Mater.* **1994**, *6*, 132–135. (b) McCullough, R. D.; Lowe, R. D.; Jayaraman, M.; Anderson, D. L. *J. Org. Chem.* **1993**, *58*, 904.

(62) Fichou, D.; Horowitz, G.; Xu, B.; Garnier, F. *Synth. Met.* **1990**, *39*, 243–259.

(63) Casper, J. V.; Ramamurthy, V.; Corbin, D. R. *J. Am. Chem. Soc.* **1991**, *113*, 600–610.

(64) (a) Bäuerle, P.; Segelbacher, U.; Maier, A.; Mehring, M. *J. Am. Chem. Soc.* **1993**, *115*, 10217–10223. (b) Yassar, A.; Delabouglise, D.; Hmyene, M.; Nessak, B.; Horowitz, G.; Garnier, F. *Adv. Mater.* **1992**, *4*, 490–493. (c) Havinga, E. E.; Rotte, I.; Meijer, E. W.; TenHoeve, W.; Wynberg, H. *Synth. Met.* **1991**, *41–43*, 473–478.